Hyperspectral imaging based detection of PVC during Sellafield repackaging procedures.

D ZABALZA, J., MURRAY, P., MARSHALL, S., REN, J., BERNARD, R. and HEPWORTH, S.

2023

Hyperspectral Imaging based Detection of PVC during Sellafield Repackaging Procedures

J. Zabalza, P. Murray, S. Marshall, J. Ren, R. Bernard, and S. Hepworth

***Abstract*—Traditionally, Special Nuclear Material (SNM) at Sellafield has been stored in multi-layered packages, consisting of metallic cans and an over-layer of plasticized Polyvinyl Chloride (PVC) as an intermediate layer when transitioning between areas of different radiological classification. However, it has been found that plasticized PVC can break down in the presence of both radiation and heat, releasing hydrochloric acid which can corrode these metallic containers. Therefore, internal repackaging procedures at Sellafield have focused recently on the removal of these PVC films from containers, where as much degraded and often adhered PVC as possible is manually removed based on visual inspection. This manual operation is time-consuming and it is possible that residual fragments of PVC could remain, leading to corrosion-related issues in future. In this work, Hyperspectral Imaging (HSI) was evaluated as a new tool for detecting PVC on metallic surfaces. Samples of stainless steel type 1.4404 – also known as 316L, the same as is used to construct SNM cans – and PVC were imaged in our experiments, and Support Vector Machine (SVM) classification models were used to generate detection maps. In these maps, pixels were classified into either PVC or 316L based on their spectral responses in the range 954-1700nm of the electromagnetic spectrum. Results suggest that HSI could be used for an effective automated detection and quantification of PVC during repackaging procedures, detection and quantification that could be extended to other similar applications.**

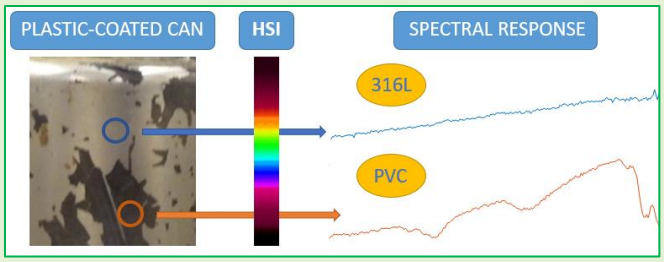

***Index Terms*—Hyperspectral imaging, PVC, repackaging, special nuclear material**

1

I. Introduction

WITHIN Sellafield's Special Nuclear Material (SNM) inventory there is a population of multi-layered packages. The packages consist of a metallic inner can, containing the SNM, and an over-layer of plasticized Polyvinyl Chloride (PVC). The inner can and PVC layer are then packed within a metallic intermediate can and finally a (breathable) stainless steel outer can. SNM packages containing PVC may deteriorate in storage. The PVC layer can degrade as a result of thermal and radiolytic effects. The degradation products (e.g., hydrochloric acid HCl) can corrode the package materials of construction. Also, the packages can pressurize as a result of gas generation during storage [1]. Both these mechanisms potentially challenge packages' structural integrity. Sellafield Ltd is currently constructing a new facility on-site, known as the Sellafield product and residue Retreatment Plant (SRP), to condition SNM packages for safe long-term storage.

Sellafield Ltd considers that this potential degradation is a significant challenge and proposes to retrieve all the PVC containing packages from the store to undertake interim remediation. The operators take the plastic-coated can out of the overpack, remove as much PVC as possible, and then reseal it in an external can. Fig. 1 shows images of an SNM can before and during the PVC removal process. The task is currently undertaken manually and a human visual inspector decides the point at which no PVC remains on the can and the cleaning process can be stopped. This translates into time-consuming, subjective, manual operations, where residual fragments of PVC could remain on the can surface with subsequent corrosion risks for the future. An automated inspection tool able to effectively detect PVC on stainless steel 316L surface to a determined, acceptable level will provide a more robust, quantitative means of determining whether a can is clean, and may reduce the potential for further HCl induced corrosion in future years, thus leading to increased storage confidence and the risk of future re-work.

Hyperspectral Imaging (HSI) is a technology able to capture an image in hundreds of different contiguous wavelengths across the electromagnetic spectrum, providing fine spectral detail of the samples under study. HSI data usually covers part of the near-infrared spectrum and can be used to characterize several physical and chemical properties of the samples under inspection to detect features that would otherwise be invisible to the human eye.

Each pixel in an HSI image contains the spectral response or

This research was funded by Sellafield Ltd and the National Nuclear Laboratory through the Game Changers Innovation Programme co-delivered by FIS360 Ltd (project GC-142).

J. Zabalza, P. Murray, S. Marshall are with Department of Electronic and Electrical Engineering, University of Strathclyde, Glasgow, G1 1XW, UK (e-mail: j.zabalza@strath.ac.uk).

J. Ren is with National Subsea Centre, Robert Gordon University, Aberdeen, AB21 0BH, UK.

R. Bernard and S. Hepworth are with Sellafield Ltd, Sellafield, Cumbria, CA20 1PG.

(a) (b)

Fig. 1. Removal of PVC coating during repackaging operations at Sellafield: (a) plastic-coated can at the start of the procedure with characteristic yellow colour due to PVC degradation, and (b) can during the removal operation showing PVC residual fragments in some areas (credit: Sellafield Ltd).

signature of the material captured by that pixel. In this context, a spectral signature, potentially unique for each material in nature, is a vector array made of hundreds of values representing the reflectance intensity for each wavelength or spectral band. With such comprehensive data, HSI technology has already been applied in a wide range of applications, including remote sensing [2], [3], food quality analysis [4], raw material classification [5], medical [6] [7], counterfeit detection [8], and others [9]-[11]. However, this technology is still expandable to many other fields. Particular applications of interest are the one proposed in [12], where HSI was used for plastic waste characterization, and the one in [13], where the same technology was used for the detection of fine metal particles in shredded electronic waste. In similar terms, HSI images could be used at Sellafield to detect PVC and residual PVC fragments on metallic surfaces, becoming a non-intrusive automated inspection tool if combined with appropriate signal and image processing algorithms and techniques.

In this work, the potential use of HSI to detect the presence of PVC on stainless steel 316L was evaluated. Experiments used real PVC and 316L samples, where a machine learning classifier known as Support Vector Machine (SVM) [14] [15] was trained to classify the image pixels – based on the spectral information they contain – into PVC or 316L, leading to detection maps which could be used for decision support in the PVC removal process. Different scenarios were tested, which included PVC samples over a 316L background and vice versa. The results demonstrated the effectiveness of HSI in discriminating PVC from 316L, detecting and quantifying its presence.

The rest of this manuscript is organized as follows: Section II describes the PVC and stainless steel 316L samples used in the experiments, along with the hyperspectral imaging system used for data acquisition and the SVM classifier implemented to obtain the detection maps. Then, Section III presents the different experiments undertaken with related results. Finally, conclusions are drawn in Section IV.

II. Materials and Methods

A. Samples

Three different types of plasticized PVC in the form of flexible films were provided by Sellafield Ltd for this study. These included not only PVC films in apparent good condition (or at least non-thermally degraded) but also PVC films thermally degraded at temperatures of 85 ºC and 100 ºC. These PVC films (see Fig. 2) were cut down into smaller pieces of different sizes for the experiments.

(a) (b) (c) (d)

Fig. 2. Types of samples used in the experiments: (a) PVC, (b) thermally degraded PVC (85 ºC), (c) thermally degraded PVC (100 ºC), and (d) stainless steel 316L mesh.

Stainless steel samples were also provided by Sellafield Ltd. These were sheets of austenitic stainless steel type 1.4404 (known as 316L) in a mesh form. This mesh structure was preferred for the experiments simply because it is easier to handle (cutting down into small items required no machinery). A 2x2cm sample of 316L mesh is shown in Fig. 2d.

B. Hyperspectral Imaging Systems

The system used to capture hyperspectral images was the RedEye 1.7 from INNO-SPEC [16] (see Fig. 3a), a camera with InGaAs detector able to acquire spectral data in the Near Infrared (NIR) range. After discarding some noisy bands inherent to the camera operation, a final range of 954-1700nm was available, covered by a total of 236 spectral bands at a spectral resolution of around 3.2nm. A system covering this spectral range was selected for PVC detection as, according to the literature, plastics exhibit clear features across the NIR range [12], [17]-[19].

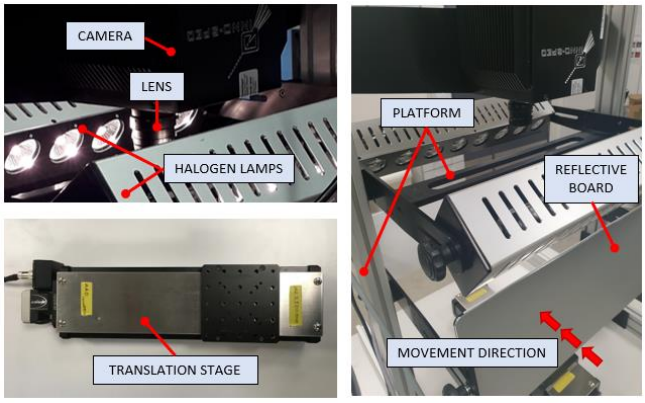

(a) (b)

Fig. 3. Hyperspectral system used in the experiments: (a) close look at camera with lens and halogen lamps (top), with translation stage to enable line scanning (bottom), and (b) overview of the system including movement direction for line scanning.

The stand-off distance between the camera and the samples was set at 50cm, leading to a spatial resolution of approximately 1mm^2 per pixel. The spatial size of the captured images varied depending on the experiment, between 60x60 and 110x190 pixels after cropping to the area of interest, i.e., the size of the scenes undergoing inspection varied between 6x6cm and 11x19cm.

The system required two sets of halogen lamps with reflective boards (see Fig. 3a) as light source for homogeneous illumination of the samples, where reflectance intensity per pixel was obtained following a standard calibration procedure with dark and white reference images [20]. This calibration used a white tile made of Spectralon for white reference, normalizing reflectance in the range [0-1] (0-black and 1-white). Images were captured by line scanning (push-broom technique [20] [21]), where the linear translational stage shown in Fig. 3 (Zolix TSA200-BF [22]) was used to introduce the relative movement between camera and samples. All images were captured indoors under the same conditions. It is worth mentioning here that deployment in the real-world would require a rotational stage applied to the can, rather than a linear stage, to line scan the surface of the cans. However, as the hyperspectral system works based on line scanning, the same approach and calibration procedure would apply.

III. Experiments and Results

A. Spectral Response of PVC and Stainless Steel 316L

The first experiment conducted was aimed at evaluating and comparing the spectral response of PVC and 316L mesh in the NIR range to ensure it would be possible to characterize and differentiate these two materials. Fig. 4 shows plots which allow a comparison between the spectral responses of 316L and PVC (the hyperspectral system captured an image of a small piece of 316L on top of a PVC layer, see Fig. 4a and 4b).

As can be seen in Fig. 4, the 316L response is relatively flat (no significant peaks) across the spectral range of the sensor, while PVC exhibits some curves around 1200nm, 1400nm, and 1650nm, which can be used to differentiate it from 316L. These findings correlate with literature, where a similar spectral response for PVC was reported [12], [17], [18], and [19], while in other work no apparent features were found for stainless steel [27].

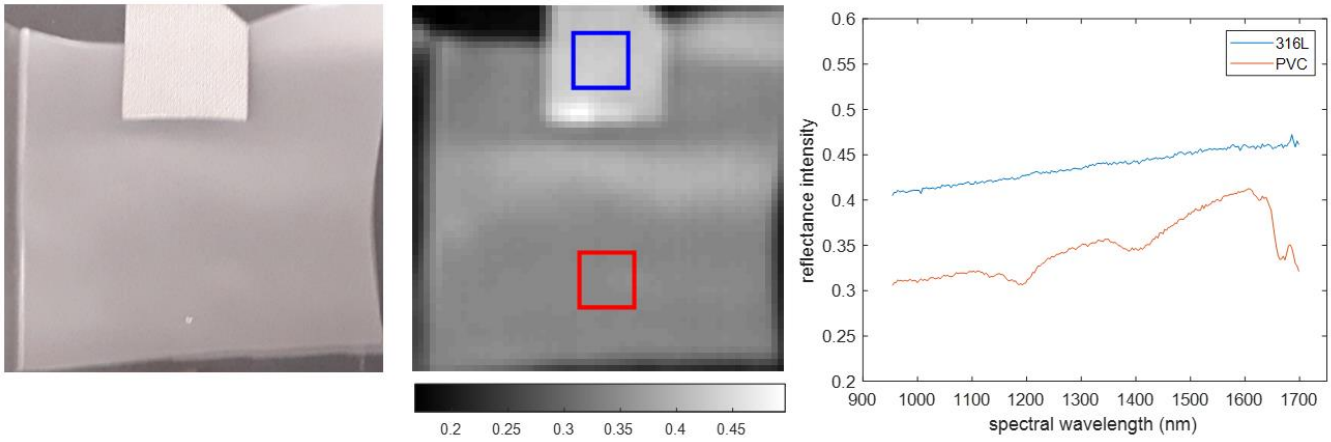

(a) (b) (c)

Fig. 4. Evaluating the spectral response of 316L and PVC: (a) conventional RGB image of the samples, (b) a single spectral band of the captured HSI image (at 1268nm, size of 60x60 pixels) highlighting two areas of 10x10 pixels (blue – stainless steel, red - PVC), and (c) spectral response of 316L and PVC from a random pixel within each area.

C. Data Classification

Detection maps indicating the presence or absence of PVC were generated by SVM [14]. This machine learning technique exploits a margin-based criterion and has been widely used for hyperspectral data classification, avoiding the curse of dimensionality or Hughes phenomenon [23]. SVM is a supervised classifier, requiring labelled samples during the training process to build an SVM model, and can be implemented by several libraries that are publicly available [24]-[26]. In this work, the popular LibSVM library [24] was selected for SVM implementation.

In the experiments, SVM used a Gaussian kernel, tuning the related 'penalty' and 'gamma' parameters by means of a grid search procedure, with an internal validation using two-fold cross-validation. An SVM model was obtained by supervised training on 316L and PVC extracted features, leading to a two-class model able to classify the pixels in the images into either PVC or 316L. Visualization, processing and classification of data were implemented in MATLAB (version R2017b), using a computer with Windows 10 (64-bit), i7 2.8GHz, 4-core, and 16GBRAM. With these specifications, the generation of detection maps required between 5-10 seconds.

B. Processing Data for Amplifying Discriminative Features

Based on the spectral responses shown in Fig. 4 of the previous section, there are some clear spectral features that could be used to distinguish PVC from stainless steel 316L. Data processing for feature extraction was implemented to exploit and amplify these features effectively, improving subsequent data analysis and automated classification by SVM.

The feature extraction proposed in this work was based on two different techniques: (i) Singular Spectrum Analysis (SSA) [28], and (ii) first derivative computation. SSA is a technique traditionally used for time-series analysis, which can decompose a 1D signal into: (i) main trend, (ii) periodic components, and (iii) noise [29]-[31]. Therefore, SSA was selected in order to remove the noise and high-frequency content from the original spectral responses [28], extracting only their main trends.

This article has been accepted for publication in IEEE Sensors Journal. This is the author's version which has not been fully edited and content may change prior to final publication. Citation information: DOI 10.1109/JSEN.2022.3221680

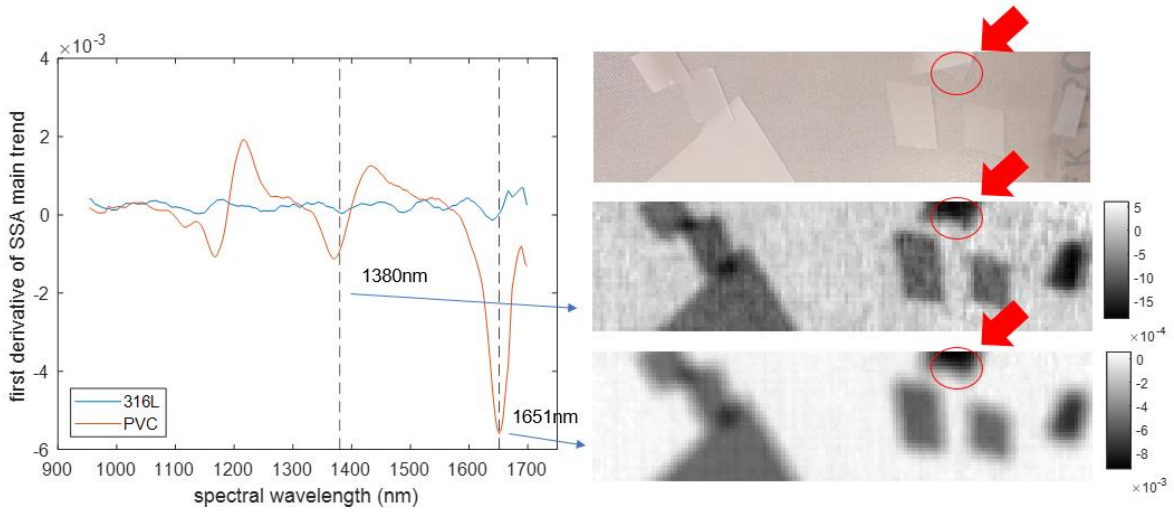

Fig. 5. Feature extraction: (a) obtained features for 316L and PVC responses, and (b) conventional RGB image of a given scene (top), with spectral images after feature extraction (size of 35x135 pixels) at 1380nm (middle), and 1651nm (bottom) to show the contrast between 316L and PVC. In these images, PVC looks darker than 316L due to the feature extraction.

SSA was configured based on [28] (window size of 10 elements, selecting the first component in the Eigenvalue decomposition). After that, the first derivative of the SSA main trends was computed to obtain the final features (this was implemented using the MATLAB 'gradient' function). The first derivative is expected to intensify those regions in which PVC and 316L become more distinct. This procedure was applied to all the pixels before undergoing classification.

Fig. 5a shows the resulting spectral responses after feature extraction for both PVC and 316L. While the 316L features are relatively flat across the NIR spectrum, PVC features present some peaks which are clearly identifiable. Fig. 5b shows a conventional RGB image containing PVC samples on top of a 316L layer (top) alongside respective spectral images from our HSI dataset at 1380nm (middle), and 1651nm (bottom) after feature extraction. As can be seen, the processed spectral images show significantly higher contrast between the 316L background and the PVC samples when compared to the RGB data. In fact, while seeing some of these PVC samples in the RGB image can be difficult (see highlighted area), they are easily visible in the spectral images.

C. Detection Maps

The resulting spectral responses after feature extraction were used to train and validate an SVM model able to classify any pixel in a hyperspectral image into either 316L or PVC. A single image (see Fig. 4) was used for training, where a 10x10-pixel area for 316L and another 10x10-pixel area for PVC were selected (after feature extraction) to train and generate the SVM model. A total of 200 pixels is a relatively small amount of training data; however, this modest training was selected to demonstrate the capabilities of the model. Significantly more training data can be gathered in future should there be a desire to adopt this technology for practical use.

Two validation experiments were carried out after training the model. In these experiments, new hyperspectral images, unseen during the training, were evaluated by the model.

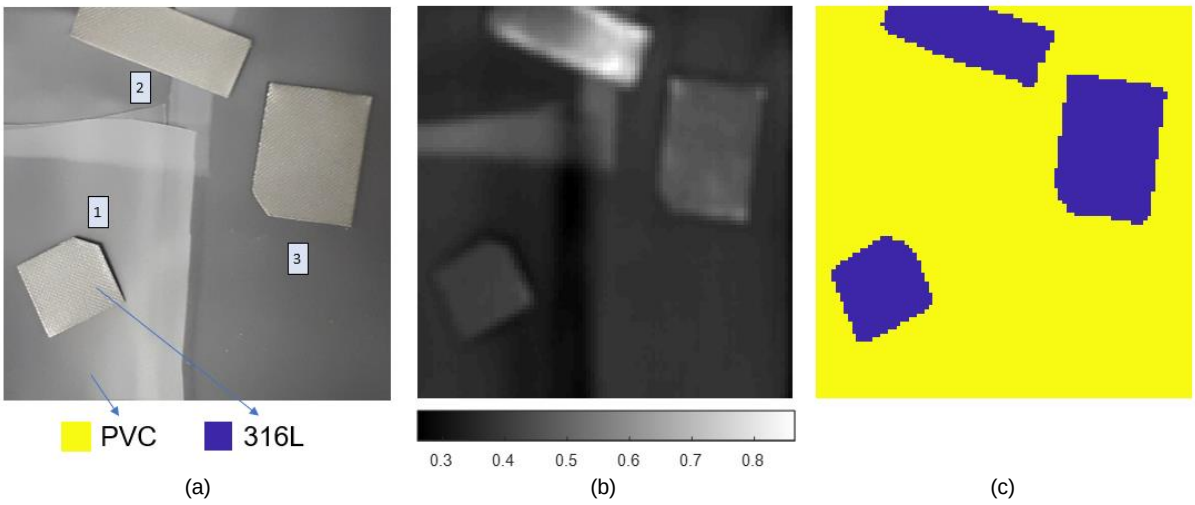

Fig. 6. Results for Experiment #1: (a) conventional RGB image for reference, (b) a spectral band (at 1268nm, size of 97x93 pixels) from the hyperspectral data, and (c) detection map (size of 97x93 pixels) where the three 316L samples were clearly detected.

This article has been accepted for publication in IEEE Sensors Journal. This is the author's version which has not been fully edited and content may change prior to final publication. Citation information: DOI 10.1109/JSEN.2022.3221680

In Experiment #1, a total of three 316L samples were placed on top of a layer of PVC (several individual PVC sheets were used to form this layer), making the PVC the background of the image acquired. In Experiment #2, 316L was used as the background of the image, where small pieces of PVC (a total of eight) were placed on top of the 316L sample. The detection maps obtained in both experiments are shown in Fig. 6 and Fig. 7.

As shown in the figures, the SVM model was able to detect the three 316L stainless steel samples in Experiment #1 (Fig. 6) and the eight PVC samples in Experiment #2 (Fig. 7), with some classification statistics available in Table I. Regardless of the size of the samples, all of them were clearly detected.

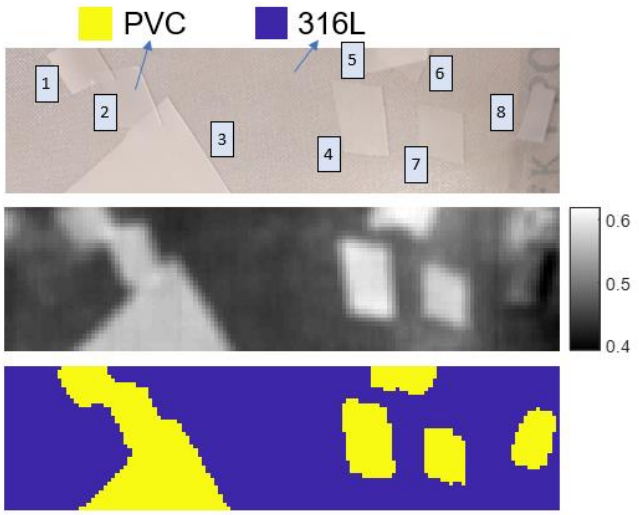

Fig. 7. Results for Experiment #2: (top) conventional RGB image for reference, (middle) a spectral band (at 1268nm, size of 35x135 pixels) from the hyperspectral data, and (bottom) detection map (size of 35x135 pixels) where eight PVC samples (some of them overlapped) were detected.

D. Spectral Response of Thermally Degraded PVC

One of the reasons why PVC coatings are being currently removed from the metallic cans is that thermal degradation of PVC under heat could be considered a corrosion agent. Therefore, during removal procedures, operators are expected to find PVC at different stages of thermal degradation. In this section, the spectral response of PVC in good condition or at least non-thermally degraded (as used in previous sections) is compared to the response of PVC thermally degraded at different temperatures (85 ºC and 100 ºC).

TABLE I
DETECTION MAP EXPERIMENTS

	Experiments	Samples detected	PVC surface	316L surface
1	316L samples on top of PVC layer	3/3	80.4% (7251 pixels)	19.6% (1770 pixels)
2	PVC samples on top of 316L layer	8/8 (overlapped)	25.4% (1201 pixels)	74.6% (3524 pixels)

Fig. 8c shows the spectral response of non-thermally degraded and thermally degraded PVC, from a random pixel within each highlighted area. As can be seen, the spectral response in the NIR range (954-1700nm) is almost identical for the three cases. Only small variations in the spectral intensity were found, but these are likely to be due to the different spatial location of the samples in the image, which slightly affects the amount of reflectance light received by the camera.

E. Detection Maps Including Thermally Degraded PVC

Final experiments included thermally degraded PVC to assess the performance of the SVM model in the presence of these degraded samples. The same model used in Experiment #1 and #2 was also used here, i.e., the model was not further trained with any thermally degraded PVC samples. The reason for this is that, according to Section III.D, the responses for thermally degraded and non-thermally degraded PVC (as used in training) are nearly identical.

In Experiment #3, a total of four 316L samples were placed on a background of PVC (layer made of several PVC sheets), and in Experiment #4, 316L was used as the background of the image again, placing small pieces of PVC (a total of eleven) on top of the 316L. Therefore, the number of samples was increased with relation to previous experiments, while the size of them was reduced to challenge the detection. PVC used here included the non-thermally degraded and thermally degraded types (at 85 ºC and 100 ºC).

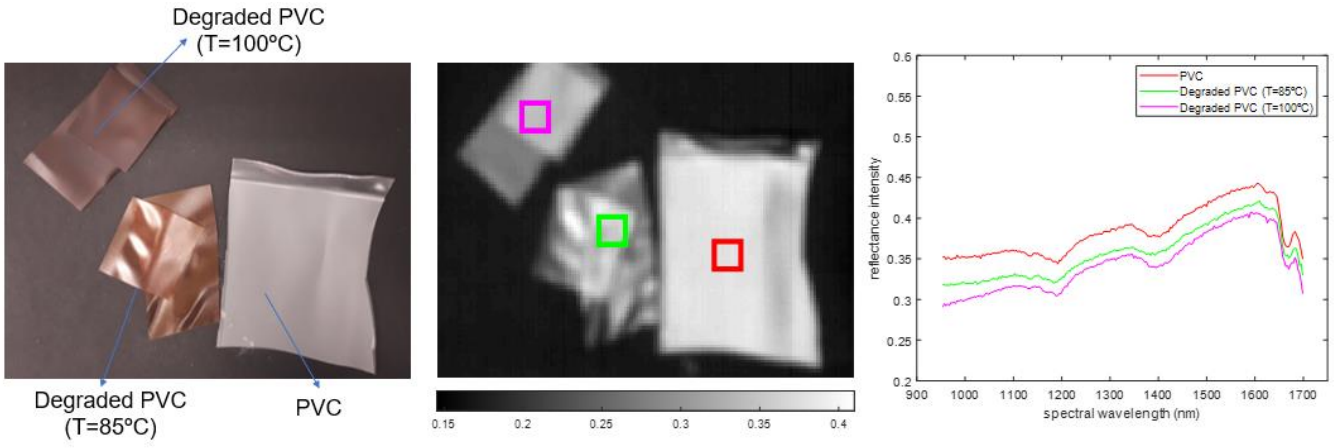

Fig. 8. Comparison of the spectral response for PVC and thermally degraded PVC: (a) conventional RGB image showing different PVC samples, (b) a spectral band (at 1268nm, size of 111x192 pixels) showing three areas in each PVC sample, and (c) spectral response from a random pixel within each area.

This article has been accepted for publication in IEEE Sensors Journal. This is the author's version which has not been fully edited and content may change prior to final publication. Citation information: DOI 10.1109/JSEN.2022.3221680

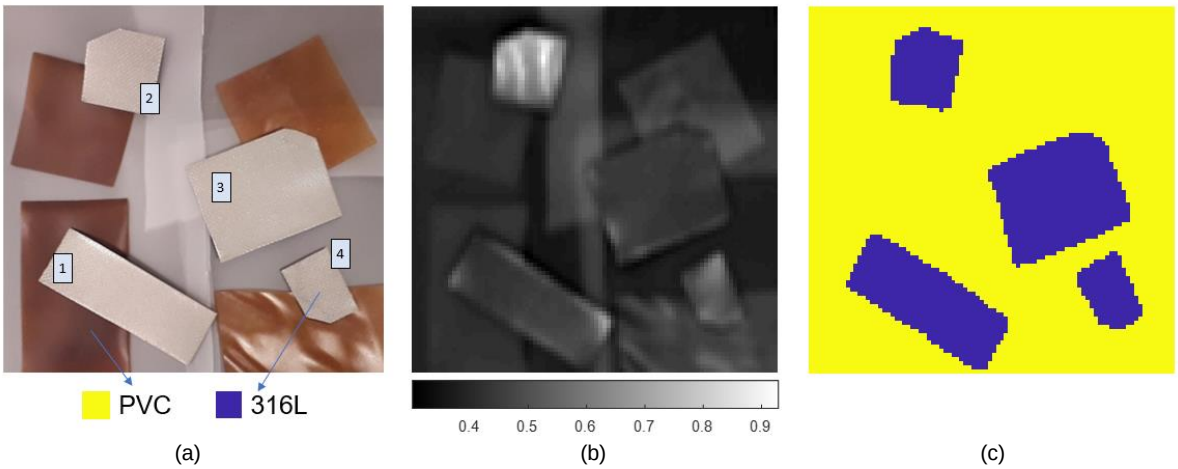

Fig. 9. Results for Experiment #3: (a) conventional RGB image for reference, (b) a spectral band (at 1268nm, size of 90x90 pixels) from the hyperspectral data, and (c) detection map where four 316L samples were detected.

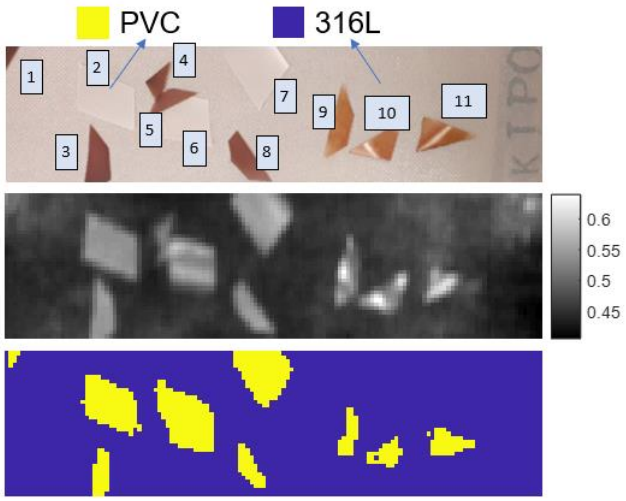

Fig. 10. Results for Experiment #4: (top) conventional RGB image for reference, (middle) a spectral band (at 1268nm, size of 36x134 pixels) from the hyperspectral data, and (bottom) detection map showing a total of eleven PVC samples (some of them overlapped), regardless of their thermally degradation.

Detection maps in Fig. 9 and Fig. 10 demonstrate the robustness of the proposed method, where all samples were detected (see Table II), even the smallest one occupying only a few pixels in the whole image (sample #1 in Experiment #4). The detection of PVC samples presented no difference regardless of their thermal degradation.

TABLE II
DETECTION MAP EXPERIMENTS INCLUDING THERMALLY DEGRADED PVC

	Experiments	Samples detected	PVC surface	316L surface
1	316L samples on top of PVC layer	4/4	76.8% (6223 pixels)	23.2% (1877 pixels)
2	PVC samples on top of 316L layer	11/11 (overlapped)	13.9% (672 pixels)	86.1% (4152 pixels)

From all the detection maps (Fig. 6-7 and Fig. 9-10), it is clear that all PVC samples were detected and highlighted, which is the main purpose of this application. However, the exact quantification of the detection accuracy in terms of number of pixels was not possible, as the available ground truth was subjective and based on human observation. Thus, a visual comparison of input and output is provided as opposed to more quantitative analysis, e.g., accuracy, precision, recall, etc., which will be the focus of future work. One of the challenges associated to this application is the spatial resolution of the hyperspectral images and the related pixel mixing effect in the boundaries of the samples. Lower resolution implies that the exact shape of the samples may be not captured accurately. However, as long as the size of the PVC samples is above the limit of detection, they will be highlighted. The resolution in this application was ~1mm^2 per pixel, which covers samples that small. Smaller limit of detection could be achieved by reducing the stand-off distance between camera and samples.

IV. CONCLUSIONS

The SNM packages containing plasticized PVC have been used at Sellafield Ltd for decades. However, when this plasticized PVC is exposed to radiation and/or heat, it degrades releasing corrosive chloride products (e.g., HCl), and Sellafield Ltd is undertaking procedures for the removal of this PVC coating. At present, these removal operations are conducted manually with the risk of missing residual PVC fragments through human visual inspection. In this work, HSI combined with intelligent signal processing has been evaluated as potential tool for automated and effective PVC detection using the spectral features of both stainless steel 316L and PVC materials for their detection and differentiation.

A hyperspectral imaging system capturing data in the NIR range (954-1700nm) was used to investigate potential features able to discriminate PVC from 316L, where key differences were found in the regions around 1200nm, 1400nm and 1650nm. These key features were processed and amplified by a feature extraction method based on the first derivative of the SSA main trend. Then, a two-class SVM model, trained on the processed features, was proven effective in distinguishing between PVC and 316L samples under diverse conditions. These conditions included different number of samples, different sample size, random location of samples, and different PVC state (non-thermally degraded PVC and thermally degraded PVC at 85 ºC and 100 ºC).

These results show that HSI could be used for effective PVC detection, quantification, and decision support in the PVC removal process. Next steps include: (i) a quantitative evaluation of the accuracy of detection (pixel-wise), (ii) moving from lab-based experiments to on-site evaluation before implementation for industrial validation, and (iii) optimizing the data acquisition and analysis processes for real-time operation.

V. References

[1] A. R. Kazanjian, P. M. Arnold, W. C. Simmons, and E. L. D'Amico, "Gas Generation Results and Venting Study for Transuranic Waste Drums," Rocky Flats Environmental Technology Site, Golden, Colorado, September 23, 1985.

[2] P. Pandey, N. Tate, and H. Balzter, "Mapping tree species in coastal Portugal using statistically segmented principal component analysis and other methods," *IEEE Sensors Journal*, vol. 14, no. 12, pp. 4434-4441, 2014.

[3] H. Sun, J. Ren, H. Zhao, Y. Yan, J. Zabalza, and S. Marshall, "Superpixel based feature specific sparse representation for spectral-spatial classification of hyperspectral images," *Sensors*, vol. 11, no. 5, 2019.

[4] S. Marshall, T. Kelman, T. Qiao, P. Murray, and J. Zabalza, "Hyperspectral imaging for food applications," in *23rd European Signal Processing Conference (EUSIPCO)*, 2015.

[5] L. Rodriguez-Cobo, P. Garcia-Allende, A. Cobo, J. Lopez-Higuera, and O. Conde, "Raw material classification by means of hyperspectral imaging and hierarchical temporal memories," *IEEE Sensors Journal*, vol. 12, no. 9, pp. 2767-2775, 2012.

[6] M. Noor, S. Salwa, J. Ren, S. Marshall, and K. Michael, "Hyperspectral image enhancement and mixture deep-learning classification of corneal epithelium injuries," *Sensors*, vol. 17, no. 11, 2017.

[7] A. Sahu, F. Saleheen, V. Oleksyuk, C. McGoverin, N. Pleshko, A. Tobarti, J. Picone, K. Sorenmo, and C.-H. Won, "Characterization of mammary tumors using noninvasive tactile and hyperspectral sensors," *IEEE Sensors Journal*, vol. 14, no. 10, pp. 3337-3344, 2014.

[8] A. Polak, T. Kelman, P. Murray, S. Marshall, D. Stothard, N. Eastaugh, and F. Eastaugh, "Hyperspectral imaging combined with data classification techniques," *Journal of Cultural Heritage*, vol. 26, 2017.

[9] V. Sudharshan, P. Seidel, P. Ghamisi, S. Lorenz, M. Fuchs, J. Fareedh, P. Neubert, S. Schubert and R. Gloaguen, "Object detection routine for material streams combining RGB and hyperspectral reflectance data based on guided object localization," *IEEE Sensors Journal*, vol. 20, no. 19, pp. 11490-11498, 2020.

[10] J. Luo, F. Cai, X. Yao, J. Li, Q. Huang, and S. He, "Experimental demonstration of an anti-shake hyperspectral imager of high spatial resolution and low cost," *IEEE Sensors Journal*, vol. 20, no. 14, pp. 8082-8090, 2015.

[11] E. Hirsh and E. Agassi, "Detection of gaseous plumes in IR hyperspectral images - performance analysis," *IEEE Sensors Journal*, vol. 10, no. 3, pp. 732-736, 2010.

[12] G. Bonifazi, F. Di Maio, F. Potenza, and S. Serranti, "FT-IR analysis and hyperspectral imaging applied to postconsumer plastics packaging characterization and sorting," *IEEE Sensors Journal*, vol. 16, no. 10, pp. 3428-3434, 2016.

[13] G. Candiani, N. Picone, L. Pompilio, M. Pepe, and M. Colledani, "Characterization of Fine Metal Particles Derived from Shredded WEEE Using a Hyperspectral Image System: Preliminary Results," *Sensors*, vol. 17, no. 5, 2017.

[14] C. Cortes and V. Vapnik, "Support vector machine," Machine Learning, vol. 20, no. 3, pp. 273-297, 1995.

[15] J. Shi, K. Cui, H. Wang, Z. Ren, and R. Zhu, "An interferometric optical fiber perimeter security system based on multi-domain feature fusion and SVM," *IEEE Sensors Journal*, vol. 21, no. 7, pp. 9194-9202, 2021.

[16] "RedEye NIR Hyperspectral Camera," [Online]. Available: https://inno-spec.de/en/redeye-1-7-en/. [Accessed Feb 2022].

[17] M. Moroni, A. Mei, A. Leonardi, E. Lupo, and F. L. Marca, "PET and PVC separation with hyperspectral imagery," *Sensors*, vol. 6, no. 5, pp. 2205-2227, 2015.

[18] H. Masoumi, S. Safavi, and Z. Khani, "Identification and classification of plastic resins using near infrared reflectance spectroscopy," *International Journal of Mechanical and Mechatronics Engineering*, vol. 6, no. 5, 2012.

[19] C. Zhu, Y. Kanaya, R. Nakajima, M. Tsuchiya, H. Nomaki, T. Kitahashi, and K. Fujikura, "Characterization of microplastics on filter substrates based on hyperspectral imaging: Laboratory assessments," *Environmental Pollution*, vol. 263, 2020.

[20] G. ElMasry and D. Sun, "Principles of hyperspectral imaging technology," Hyperspectral imaging for food quality analysis and control. Academic Press, pp. 3-43, 2010.

[21] J. Zabalza, J. Ren, and S. Marshall, "'On the fly' dimensionality reduction for hyperspectral image acquisition," in *23rd European Signal Processing Conference (EUSIPCO)*, 2015.

[22] "Zolix Translational stage," [Online]. Available: http://www.zolix.com.cn/en/prodcon_371_384_418_464.html. [Accessed Feb 2022].

[23] G. Hughes, "On the mean accuracy of statistical pattern recognition," *IEEE Transactions on Information Theory*, Vols. IT-14, no. 1, pp. 55-63, 1968.

[24] C.-C. Chang and C.-J. Lin, "LIBSVM: a library for support vector machines," *ACM Transactions on Intelligent Systems and Technology*, vol. 2, no. 3, 2011.

[25] T. Joachims, "SVMlight," [Online]. Available: https://www.cs.cornell.edu/people/tj/svm_light/. [Accessed February 2022].

[26] R. Collobert and S. Bengio, "SVMTorch," [Online]. Available: https://bengio.abracadoudou.com/SVMTorch.html. [Accessed February 2022].

[27] J. Jyothi, A. Biswas, P. Sarkar, A. Soum-Glaude, H. Nagaraja, and H. Barshilia, "Optical properties of TiAlC / TiAlCN / TiAlSiCN / TiAlSiCO / TiAlSiO tandem absorber coatings by phase-modulated spectroscopic ellipsometry," *Applied Physics A*, vol. 123, no. 496, 2017.

[28] J. Zabalza, J. Ren and S. Marshall, "Singular spectrum analysis for effective noise removal and improved data classification in hyperspectral imaging," in *IEEE WHISPERS*, 2014.

[29] N. Golyandina and A. Zhigljavsky, Basic SSA, Berlin: Springer, 2020.

[30] J. Zabalza, J. Ren, Z. Wang, H. Zhao, J. Wang, and S. Marshall, "Fast implementation of singular spectrum analysis for effective feature extraction in hyperspectral imaging," *IEEE Journal of Selected Topics in Earth Observation and Remote Sensing*, vol. 8, no. 6, pp. 2845-2853, 2015.

[31] J. Zabalza, C. Qing, P. Yuen, G. Sun, H. Zhao and J. Ren, "Fast implementation of two-dimensional singular spectrum analysis for effective data classification in hyperspectral imaging," *Journal of the Franklin Institute*, vol. 355, no. 4, pp. 1733-1751, 2018.

Jaime Zabalza (Member, IEEE) received the M.Eng. degree in industrial engineering from the Universitat Jaume I (UJI), Castellón, Spain; and the M.Sc. and Ph.D. degrees in Electronic and Electrical Engineering from the University of Strathclyde, Glasgow, U.K. He was awarded the IET Image & Vision Section prize for best Ph.D. thesis for his work in hyperspectral remote sensing.

He is currently a Chancellor's Fellow (Lecturer), within the Advanced Nuclear Research Centre (ANRC) at the Department of Electronic and Electrical Engineering, University of Strathclyde. His research interests include hyperspectral data analysis as well as signal and image processing in a wide range of applications.

Paul Murray received the M.Eng. and Ph.D. degrees in Electronic and Electrical Engineering from the University of Strathclyde, Glasgow, U.K., in 2008 and 2012, respectively.

He is a Reader at the University of Strathclyde in the department of Electronic and Electrical Engineering. His research interests include image processing, hyperspectral imaging & analysis, feature extraction, machine learning and artificial intelligence.

This article has been accepted for publication in IEEE Sensors Journal. This is the author's version which has not been fully edited and content may change prior to final publication. Citation information: DOI 10.1109/JSEN.2022.3221680

Stephen Marshall (Senior Member, IEEE) received a first class honours degree in Electrical and Electronic Engineering from the University of Nottingham and a PhD in Image Processing from University of Strathclyde.

He has been a Professor at University of Strathclyde since 2006. His research activities have been focused in the area of Non Linear Image Processing. In this time, he has pioneered new design techniques for morphological filters based on a class of iterative search techniques known as genetic algorithms. The resulting filters have been applied as four-dimensional operators to successfully restore old film archive material.

In recent years he has established the Hyperspectral Imaging Centre at the University of Strathclyde. The aims to provide solutions to industrial problems through applied research and Knowledge Exchange.

He has published over 200 conference and journal papers on these topics including IET, IEEE, SPIE, SIAM, ICASSP, VIE and EUSIPCO. He has also been a reviewer for these and other journals and conferences.

He is a Fellow of the Institution of Engineering and Technology (IET) and a Senior member of the IEEE. He has also been successful in obtaining research funding from National, International, and Industrial sources. These sources include EPSRC, EU, BBSRC, NERC and Innovate UK.

Stephen Marshall is also the lead academic for the Vertically Integrated Project Program.

Jinchang Ren (Senior Member, IEEE) received his B. Eng. degree in computer software, M.Eng. in image processing, and D. Eng. in computer vision, all from Northwestern Polytechnical University, Xi'an, China. He was also awarded a Ph.D. degree in Electronic Imaging and Media Communication from the University of Bradford, Bradford, U.K.

Currently he is a full Professor of Computing Sciences, Transparent Ocean Lead, and Director of the Hyperspectral Imaging Lab at the National Subsea Centre (NSC), also Director of NSC International PGR Academy, Robert Gordon University, Aberdeen, U.K.

Jinchang is a Senior Member of IEEE, and Lifetime Achievement Fellow of Marquis Who's Who. His research interests focus mainly on hyperspectral imaging, image processing, computer vision, big data analytics and machine learning, with a research portfolio over £6 million. He has published 300+ peer reviewed journal/conferences articles, and acts as an Associate Editor for several international journals including IEEE TGRS and J. of the Franklin Institute et al. He has also chaired and co-chaired a number of conferences and workshops. His students have received many awards, such as the Best PhD thesis from IET Image and Vision Section (for Jaime Zabalza's work in hyperspectral image analysis) in 2016 and various conferences/workshops.

Robert Bernard is a Senior Technology Manager at Sellafield Ltd. He leads at team of scientists and engineers specialised in the safe storage and management of Special Nuclear Materials on the Sellafield site.

To achieve this, Robert works closely with his team to engage with the academic community and industrial partners in the Sellafield supply chain to ensure that he and his team have the best technology and expertise (internally and within the supply chain) to ensure he can continue to effectively inspect, monitor, and keep-safe the SNM products for which he and his team are responsible.

Steve Hepworth (University Lead, Sellafield Ltd, UK) gained a BSc (hons) in Applied Physics (UCLAN) 1995, an MSc in Medical Physics (Aberdeen) 1996 and a PhD in Medical Radiation Physics (Surrey) in 2000.

He has over 20 years of experience in the civil nuclear industry, initially specializing in radiation measurement techniques on legacy infrastructure and operational reprocessing plants. His last 15 years at Sellafield Ltd have been spent in Nuclear Decommissioning R&D during which time he has designed and commissioned studies on a variety of decommissioning projects including remote cutting methods, novel radiometric monitoring, unmanned aerial vehicles, hydrogen detection, energy harvesting, decontamination and virtual environments. During this time, he also led a multi-disciplinary team examining methods of detecting and mitigating leaks from the Magnox Swarf Storage Silo.

Steve is now a part of the senior leadership team in science and technology at Sellafield Ltd with the responsibility of developing University relationships and collaborations. He is a Chartered Physicist and Fellow of the Institute of Physics.